January 1985 LRP 257/85

THE PHASE CONTRAST TECHNIQUE AS AN IMAGING DIAGNOSTIC FOR PLASMA DENSITY FLUCTUATIONS

H. Weisen

The Phase Contrast Technique as an Imaging Diagnostic for Plasma Density Fluctuations

Henri Weisen
Centre de Recherches en Physique des Plasmas
Association Euratom - Confédération Suisse
Ecole Polytechnique Fédérale de Lausanne
21, Av. des Bains, CH-1007 Lausanne, Switzerland

ABSTRACT

The phase contrast technique offers an attractive alternative to small angle Thomson scattering for the investigation of plasma density fluctuations. This imaging technique converts small relative phase shifts into detectable intensity variations.

A wave optics treatment is given and test results of a system built for the TCA tokamak are presented. The device is suitable for the study of density fluctuations in the wavelength range from 2 to 200 mm. It uses a low power continuous CO_2 laser probe beam of 15 cm width and liquid nitrogen cooled HgCdTe detectors. For a 1 MHz bandwidth it allows detection of phase shifts as low as $3 \cdot 10^{-6}$ radians at the shot noise limit, corresponding to relative density variations $\Delta n_e/n_e \simeq 10^{-4}$ for typical conditions on TCA.

1. Introduction

Electron density fluctuations in magnetically confined plasmas, like drift wave turbulence, have mainly been investigated using far field scattering techniques [1,2]. The difference of the approach described here is that it is an imaging technique similar to imaging interferometry that provides information that is spatially rather than wave number resolved. This is a potential advantage, particularly at long fluctuation wavelengths, where wavenumber resolution conflicts with spatial resolution.

Most of the low frequency fluctuations of interest in a tokamak plasma seem to fall into a wavelength range from a few millimeters to several centimeters [1,2,6]. At these long wavelengths, diffraction occurs in the Raman-Nath regime rather than in the Bragg regime when the probe wavelength is 10.6 μm [4]. Therefore the plasma with its fluctuations acts like a weak, thin phase object, causing small phase shifts ($|\phi| \ll 1$ radian), given by the usual line integral of the refractive index $n_{(\underline{x},z,t)}$:

$$\phi(\underline{x},t) = 2\pi/\lambda \int (n_{(\underline{x},z,t)}-1)dz \qquad (1)$$

with $\underline{x} = (x_1, x_2)$

or $\phi(\underline{x},t) = -2.81 \cdot 10^{-13} \lambda N_e(\underline{x},t)$

where λ is the wavelength in centimeters of the probe beam propagating along z

$$N_{e(\underline{x},t)} = \int n_{e(\underline{x},z,t)}dz \qquad [cm^{-2}]$$

and n_e is the electron density $[cm^{-3}]$

Thus the effect of the plasma on the transmitted wavefront is fully described by $\phi(\underline{x},t)$ and its measurement is most naturally performed by interferometry or a related technique, like phase contrast.

2. The principle of the phase contrast technique

The phase contrast method [10], invented in 1935 by Zernike, has to our knowledge only been applied by one group to investigate plasmas using a pulsed ruby laser [5].

In the basic setup (Fig. 1) a parallel beam of (laser) radiation is transmitted through the test object, a weak, thin phase object in the plane Σ and focussed onto an optical filter P, called the phase plate (or phase mirror if it is a reflective device), by lens L_1. The undiffracted light (UD, diffraction order 0) is focussed onto the depressed region of P (the conjugate area) causing it to be phase shifted by $\pi/2$ with respect to diffracted light (D) falling beside it (on the complemetary area). This operation causes phase shifts to be revealed as intensity variations in the image plane Σ'.

For an incident plane wave of unit amplitude, the transmitted amplitude can be written as

$$A_{(\underline{x},t)} = \exp\left(i\phi_{(\underline{x},t)}\right) \approx 1 + i\phi_{(\underline{x},t)} \quad \text{for } |\phi| \ll 1.$$

The amplitude in the focal plane of L_1 is a scaled version of the Fourier transform $\tilde{A}_{(\underline{k},t)}$ of $A_{(\underline{x},t)}$ with $k = 2\pi y/\lambda f_1$, y being the distance to the optical axis:

$$\tilde{A}_{(\underline{k},t)} = \delta(\underline{k}) + i\tilde{\phi}_{(\underline{k},t)}$$

$\tilde{\phi}_{(\underline{k},t)}$ is the diffracted part, and ideally the action of the phase plate is to phase shift it by $\pi/2$ without affecting the undiffracted part $\delta(\underline{k})$:

$$\tilde{A}'_{(\underline{k},t)} = \delta(k) + \tilde{\phi}_{(\underline{k},t)} \quad .$$

Lens L_2 then performs the inverse transform:

$$A'_{(\underline{x},t)} = 1 + \phi_{(\underline{x},t)} \quad .$$

The detected intensity $\left| A'(\underline{x},t) \right|^2$ now contains a term that is linear in $\phi(\underline{x},t)$:

$$\left|A'(\underline{x},t)\right|^2 \simeq 1 + 2\,\phi(\underline{x},t)$$

$$\text{i.e. } I(\underline{x},t) \simeq I_0(\underline{x},t)\,\left(1 + 2\,\phi(\underline{x},t)\right) \qquad (2)$$

where $I(\underline{x},t)$ and $I_0(\underline{x},t)$ are the intensities in the presence and in the absence of $\phi(\underline{x},t)$ respectively.

Clearly the conjugate area must be at least as wide as the focal spot size, and only the diffracted light falling beside it (with a sufficiently large angle of diffraction) will contribute to the intensity variations of eq. (2). Thus, the instrument is a spatial high pass device.

3. Transfer properties

The theoretical framework used to analyse optical filtering techniques such as this can be found in [3]. Let $B(x)$ be the probe beam amplitude profile in Σ. For $|\phi| \ll 1$ the transmitted beam is:

$$B'(x,t) = (1 + i\phi(x,t))\, B(x) \qquad (3)$$

Dropping the time dependence of $\phi(x,t)$, the amplitude in the focal plane of L_1 is

$$\tilde{B}'(k) = (\delta(k) + i\tilde{\phi}(k)) \circledast \tilde{B}(k) \qquad (4)$$

where $\sim$ designates Fourier transforms and $\circledast$ the convolution operation. Even though x and k are taken to be scalars for convenience, formally the calculations are valid for two dimensions. The phase plate modifies this complex amplitude as follows:

$$\tilde{B}''(k) = [1-(1+i)\,\tilde{C}(k)]\tilde{B}'(k) \qquad (5)$$

$\tilde{C}(k)$ delimits the conjugate area extending from $-k_c$ to $+k_c$. It takes the value 1 within this interval and 0 outside. The inverse transform of (5) provides the amplitude in Σ' except for the

magnification factor $m = f_2/f_1$:

$$B''_{(x)} = R_{(x)} + D_{(x)}$$

$$\text{where } R_{(x)} = B_{(x)} - (1+i)B_{(x)} \circledast C_{(x)} \tag{6}$$

$$\text{and } D_{(x)} = i\phi_{(x)}B_{(x)} + (1-i)\left(\phi_{(x)}B_{(x)}\right) \circledast C_{(x)}.$$

$C_{(x)}$ is the inverse Fourier transform of $\tilde{C}_{(k)}$. The amplitude distribution $B''_{(x)}$ leads to the detectable intensity distribution

$$I_{(x)} = \left|B''_{(x)}\right|^2$$

$$= \left|R_{(x)}\right|^2 + R_{(x)}\, D^*_{(x)} + R^*_{(x)}D_{(x)} + \left|D_{(x)}\right|^2. \tag{7}$$

The $R_{(x)}D_{(x)}$ interference terms are linear in $\phi_{(x)}$ and describe the intensity variations due to $\phi_{(x)}$. $R_{(x)}$ acts as a local oscillator for the homodyne detection of $D_{(x)}$. The term $\left|D_{(x)}\right|^2$ is of the order ϕ^2 and therefore negligible when $|\phi| \ll 1$.

From (7) we find for the homodyne intensity variations

$$\Delta I_{(x)} = R_{(x)}D^*_{(x)} + R^*_{(x)}D_{(x)}$$

$$= 2\left[B_{(x)} \circledast C_{(x)}\right] \phi_{(x)}B_{(x)} - 2B_{(x)}\left[\left(\phi_{(x)}B_{(x)}\right) \circledast C_{(x)}\right] \tag{8}$$

In equation (8), $\Delta I_{(x)}$ essentially depends on the difference between $\phi_{(x)}$ and a weighted average of $\phi_{(x)}$ over neighboring points, $C_{(x)}$ being the weighting function. This suggests the designation of "internal reference interferometer" for a phase contrast device. Equation (8) leads back to (2) when the conjugate area width is both large enough to collect virtually all of the undiffracted and small enough to collect none of the diffracted light.

Over an area where $B_{(x)}$ is roughly constant, the system can be considered to be shift invariant, and can therefore be characterized by its transfer function (wavenumber response function) obtained from eq. (8):

$$H_{(k)} \quad \alpha \quad \left| 1 - \frac{B_{(k)} \circledast C_{(k)}}{B_{(\ell)} \circledast C_{(\ell)}} \right|_{\ell = 0} \tag{9}$$

Eq.(9) states that for a sinusoidal perturbation of wavenumber k the amplitude of the intensity modulations is proportional to the fraction of diffracted light striking the complementary area. Thus when k_c is matched to the diffraction limited focal spot size, the device becomes sensitive to fluctuations with wavelength of the order of the diameter of the beam passing through the plasma.

4. Experimental setup on the TCA tokomak

One of the main motivations for the development of this diagnostic is to study the resonant layer(s) occuring during Alfvén wave heating. Mean radial wavelengths of several centimeters are expected (6). The technique allows one to discriminate between the long wavelength global Alvén eigenmodes and the shorter wavelength resonant layer fluctuations by setting the instrument's cutoff wavelength to an intermediate value. In addition it will allow the study of plasma turbulence and its relevance to plasma confinement. Density fluctuations associated with magnetic islands and relaxation oscillations will also be observable.

Access to the plasma is allowed by a pair of elongated NaCl windows (W) with 23 x 4 cm clear aperture extending from the outer plasma edge to beyond its minor axis (fig. 2). The continuous CO_2 waveguide laser producing 8 Watts and the expanding and collimating optics (not shown) are mounted on the rear side of a vertical optical table. The main beam is a rectangular section chopped out of a gaussian beam of $1/e^2$ diameter of $\approx$ 15 cm (adjustable). The beam processing optics which include the focussing mirror L_1 (f_1=190 cm), the imaging mirror L_2 (f=27.5 cm) and the phase mirror P are on the front side. For beam profile scans a rotating mirror R and an auxiliary lens L are available. The nitrogen cooled HgCdTe detectors may be in the

planes Σ' or Σ'', both being conjugate to Σ. With the present design parameters the shot noise limited sensitivity for a S/N ratio of 1 is $\phi_{min} \simeq 3.10^{-6}$ radians for a 1 MHz bandwidth. If an effective integration depth of 4 cm is assumed this corresponds to $\Delta n_e/n_e \simeq 10^{-4}$ for typical conditions in the TCA tokamak. Estimates based on scattering results [1,2] for other tokamaks yield values of several centimeters for the effective integration depth in the case of plasma turbulence.

The usual rigid C-bracket of an interferometer is not needed because the instrument is insensitive to absolute path length variations. Beam deflections are avoided by mounting three relay mirrors RM (only two shown, fig. 2) at right angles to each other (as in a corner cube reflector) into rigid boxes that are independently vibration isolated. This allows a space and weight saving construction as compared to an interferometer, and is also less sensitive to mechanical perturbations. It is designed to allow the study of fluctuations transverse to the magnetic field with wavelength up to 20 cm, which is far longer than is accessible by current scattering techniques, most of which use probe beams with a diameter of the order of only 1 cm.

Three phase mirrors were made by overcoating flat steel mirrors with a 1.4 μm thick Al-layer whilst repectively 120, 200, 350 μm wide wires were stretched across them as masks to produce corresponding width grooves (conjugate areas). At an incidence angle of 20 ° they produce the desired 90 ° phase shift between undiffracted light focussed into the groove and diffracted light falling beside it. They withstand at least 3 Watts of CO_2 laser power focussed onto a 170 μm wide spot without damage.

5. Test results

Our initial concern was to check if the system, which is scheduled for installation on TCA in autumn 1984, is able to achieve the desired diffraction limited response to wavelengths up to about 20 cm.

A convenient way to determine the wavenumber response experimentally was to first measure the system's response to a small phase step produced by inserting in Σ a 12 μm thick, almost transparent Mylar sheet covering half of the object plane. By a suitable choice of its inclination it produced phase shifts of $2\pi \pm 0.1$ radians.

The rotating mirror was used to scan the intensity profile in plane Σ''. The continuous trace (I^+) in fig. 3 shows the effect of the slight positive phase step and the broken trace that of the negative step (I^-). The conjugate area width was 200 μm. Each curve is averaged over 5 digitized oscilloscope traces to reduce the effect of air convection in the beam path, to which the instrument is also sensitive.

From eq. (2):

$$\Delta\phi \approx 0.5(I^+-I^-)/(I^+ + I^-) = 0.5\ \Delta I/I$$

The step is correctly reproduced in the immediate vicinity of the discontinuity, but its effect settles down to zero at some distance from it, as expected in a spatial high pass device. In fig. 3 the Mylar sheet was on the right side, which is therefore also affected by imperfections of the latter. Fig. 4 shows the relative intensity variations $\Delta I/I$ of the left side only and represents the step response of the system for w = 200 and 350 μ respectively. From these step responses, the transfer functions were obtained by dividing their Fourier transforms (512 points FFT) by that of a step function (fig. 5). The observed cutoff wavelengths were $\Lambda_c = 2\pi/k_c \approx 19$ cm and

$\Lambda_c \simeq 12$ cm respectively, the expected values being 20 and 11.5 cm. With the calculated focal spot size being 170 μm ($1/e^2$), the phase plate with w = 120 μm was underdimensioned leading to strong alterations of the original intensity profile, such that (2) was not applicable. The system was however clearly sensitive to wavelength up to about 30 cm.

The two little humps on fig. 3 result from the filtering action of the phase mirror and mark the limiting aperture of the optics cutting the originally gaussian beam.

With our system we were able to detect sound waves in the frequency range ν = 0.3 to 17 kHz (115 cm > Λ > 2 cm) produced by a loudspeaker directed transversely across the beam. The detector was in Σ'. This approach seems to be less reliable for obtaining the transfer function because it depends on an acoustic calibration of the loudspeaker and on the integration length that is a function of the emission pattern of the speaker. A simple analytical model of a diverging wavefield suggests

$$\Delta\phi(x,t) = 2\pi/\lambda \int \Delta n_{(x,z,t)} dz \simeq 2\pi/\lambda \; \Delta n_{(x,z=o,t)} \; L \; ,$$

where $\Delta n_{(x,z,t)}$ is the refractive index perturbation due to a spherical sound wave and

$L = \sqrt{R\Lambda} = \sqrt{2\pi R/k}$ is the effective integration depth.

R = 1m is the radius of curvature of the acoustic wavefront at the point viewed.

For each wavenumber $k = 2\pi\nu c$, c being the speed of sound in air, the amplitudes of the intensity modulations detected were normalized to the sound pressure previously measured with a calibrated microphone and to their respective integration depths. Fig. 6 shows the result for w = 350 μm, which is in reasonable agreement with the step response measurements.

6. Discussion

We now compare this technique with other optical plasma density (fluctuation) diagnostics.

The usefulness of scattering techniques [1,2] for tokamaks is restricted at long wavelengths to a fraction of the plasma radius, (usually less than a few centimeters) by the combination of two conditions: 1) The viewed volume should represent a homogeneous plasma sample, and 2) for adequate wavenumber resolution it must be larger than the longest wavelength to be studied [7]. When these conditions cannot be satisfied the spatially resolved data from an imaging diagnostic will be more relevant. Thus scattering appears to be adequate from the smallest fluctuation wavelength to at most a few centimeters, and imaging techniques are adequate for wavelength allowing an interpretation according to eq. (1), i.e. for typical wavelengths above a few millimeters when a CO_2 laser is used (i.e. in the Raman-Nath case).

If only fluctuations are to be studied, no absolute phase difference measurement is required and this imaging technique does not need to be a conventional interferometer. It can be made to generate its reference internally as discussed above. Thus the effect of mechanical vibrations is automatically compensated, allowing a simpler and more compact construction than would be possible with a conventional interferometer. This is an important feature because of the limited space available for diagnostics around a tokamak.

The phase contrast device developed for TCA is designed for a flat "interferometer-like" response in the wavelength range from about 2 mm to 20 cm. Other imaging techniques can be envisaged, however this particular concept has the merit of a transfer function coming closest

to the wavenumber independent transfer function of an interferometer, and is therefore easiest to interpret.

Clearly for the most global scales (density profile measurements) interferometers using an external reference beam are required [8,9]. Phase contrast has the potential of bridging the gap between these scales and those traditionally investigated by scattering.

The retrieval of local quantities from a line integrated measurement (eq. 1) is a difficulty the phase contrast technique shares with many other optical plasma diagnostics including small angle scattering and interferometry. In the case of fluctuations it will generally rely on particular models or symmetry assumptions about $\Delta n_{(x,z,t)}$ or its statistical properties.

Conclusion

The phase contrast technique can provide a simple and compact diagnostic for a broad spectrum of plasma density fluctuations. The performance of the system designed for the TCA tokamak has experimentally been shown to be equivalent to that of an imaging interferometer for wavelengths up to about 20 cm, with the advantage of being lightweight and less sensitive to mechanical perturbations. The range of accessible wavelength is considerably wider than which can be studied by scattering techniques.

Acknowledgements:

The author thanks Dr. R. Behn, Dr. M. Siegrist, Dr. J. Lister (CRPP) and Dr. P.D. Morgan (JET) for many helpful discussions and suggestions.

FIGURE CAPTIONS

Fig 1 : Basic setup for phase contrast. Σ: object plane. Σ': image plane. P: phase plate. D: diffracted light component (thin lines). UD: undiffracted light component, L_1 and L_2: focussing and imaging lenses.

Fig 2 : Experimental setup

Σ: object plane centered on the plasma midplane. Σ', Σ'': image planes of the plasma. W: NaCl windows. RM: relay mirrors. L_1: main parabolic mirror. P: phase mirror. L_2: imaging mirror. L: auxiliary lens. R: rotating mirror. The beam producing optics on the rear side of the table use a mirror identical to L_1 and a ZnSe expanding lens.

Fig 3: Measured effect on the intensity profile of small step-like phase discontinuities. Solid line: positive step (I^+), broken line: negative step (I^-).

Fig 4: Step responses for conjugate area widths w = 200 μm and w = 350 μm.

Fig 5: Transfer functions obtained from the step responses of fig 4.

Fig 6: Normalized response of the system to acoustic waves in the range 0.3 - 17 kHz.

REFERENCES

[1] Slusher R.E. and Surko C.M., Phys. Fluids 23, 472 (1980).

[2] Evans D.E., Doyle E.J., Frigione D., von Hellermann M. and Murdoch A., Plasma Physics 25, 619 (1983).

[3] Gaskill D., Linear Systems, Fourier Transforms and Optics, John Wiley & Sons, New York (1978).

[4] Weisen H., "Optical filtering techniques applied to the study of collective density fluctuations in plasmas", CRPP internal report INT 108/82, Lausanne (1982).

[5] Presby H.M. and Finkelstein D., Rev. Sci. Instruments 38, 1563 (1967).

[6] Ross D.W., Chen G.L. and Mahajan S.M., Phys. Fluids 25, 652 (1982).

[7] Holzhauer E. and Massig J.H., Plasma Physics 20, 867 (1977).

[8] Véron D., Submillimeter Interferometry of High-Density Plasmas, in : Infrared and Millimeter Waves, Vol. 2, p. 67, K.J. Button, Academic Press, New York (1979).

[9] Hugenholtz C.A.J. and Meddens B.J.H., Rev. Sci. Instruments 53, 171 (1982).

[10] Born M. and Wolf E., "Principles of Optics" p. 424, Pergamon Press, Oxford (1975).

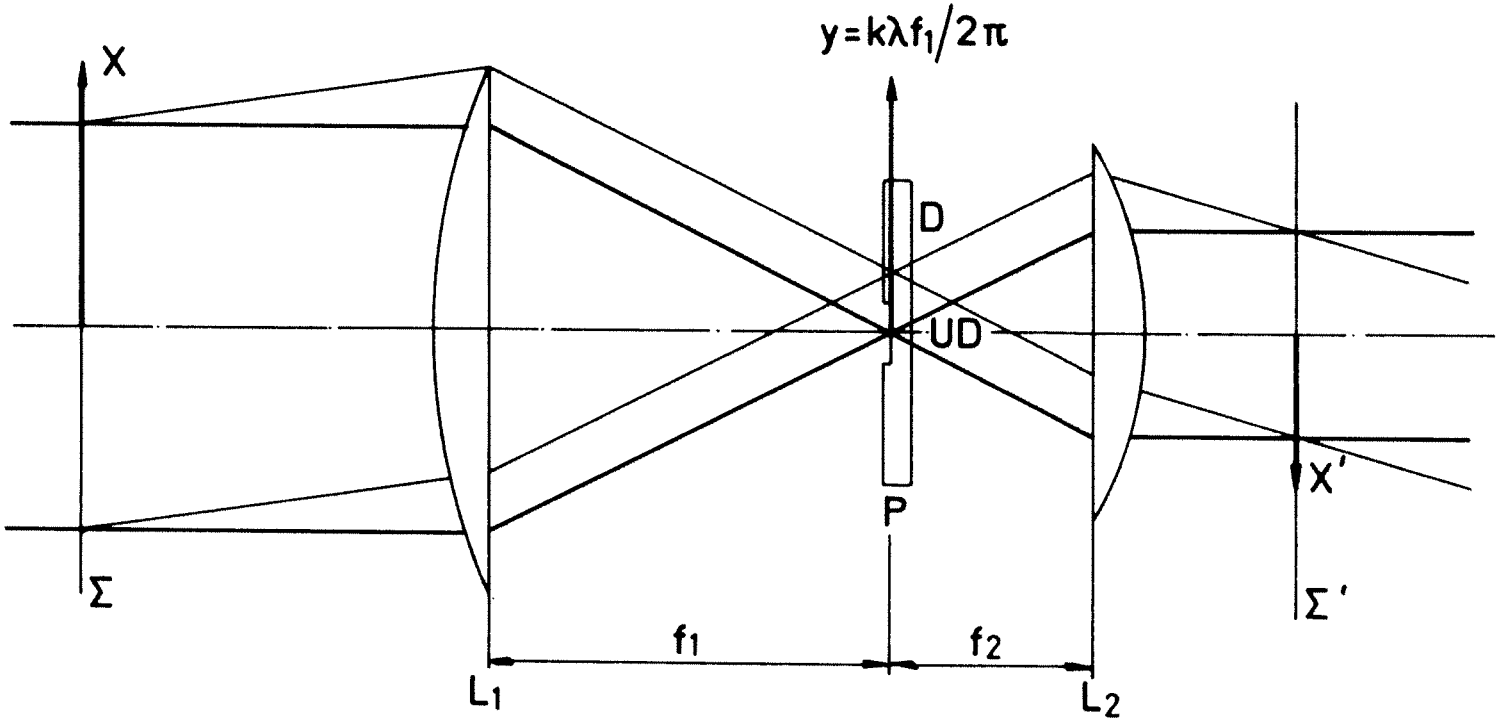

fig. 1

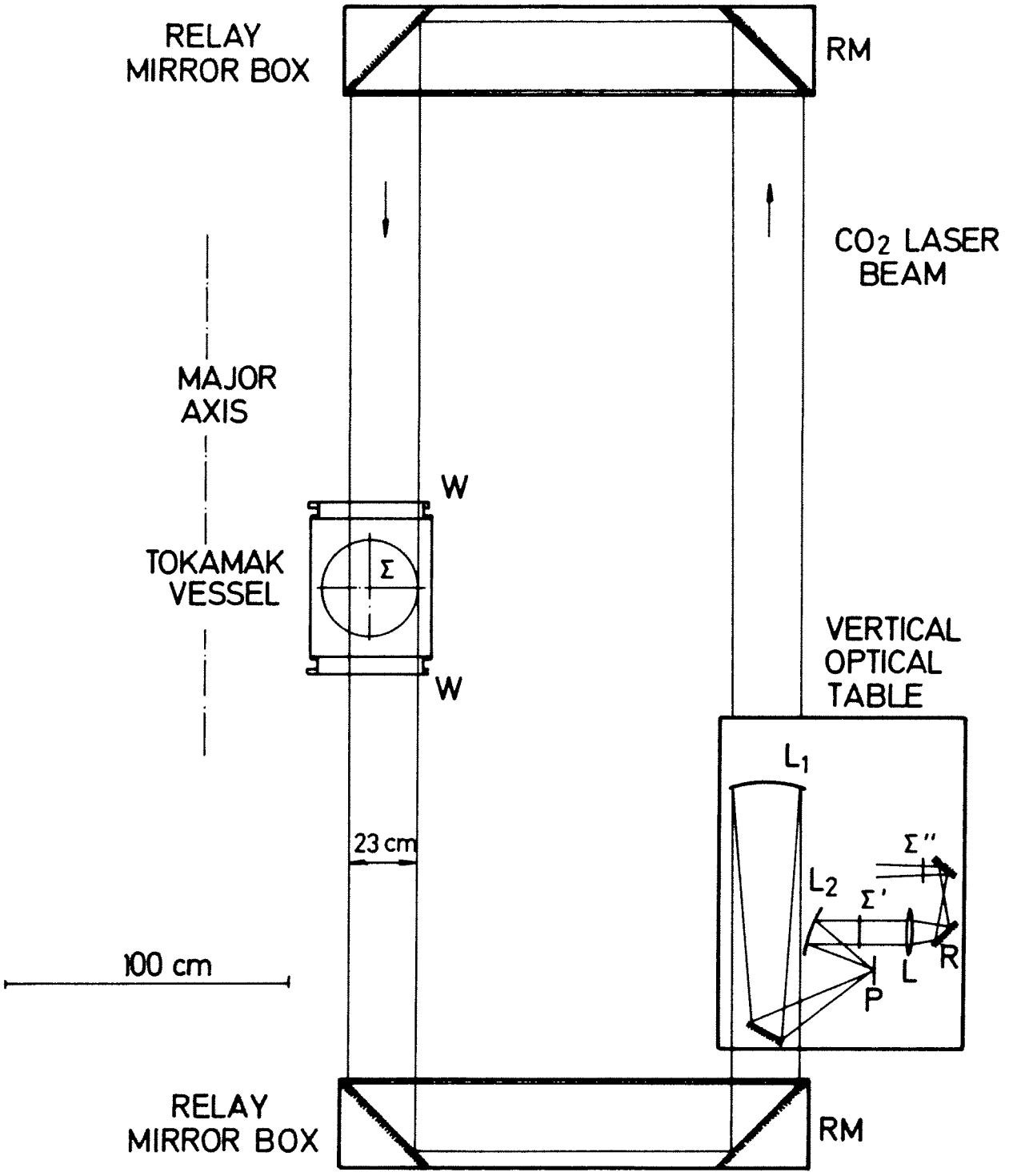
RELAY
MIRROR BOX
RM
CO2 LASER
BEAM
MAJOR
AXIS
W
TOKAMAK
VESSEL
Σ
W
VERTICAL
OPTICAL
TABLE
L1
23 cm
Σ''
L2
Σ'
R
L
P
100 cm
RELAY
MIRROR BOX
RM

fig. 2

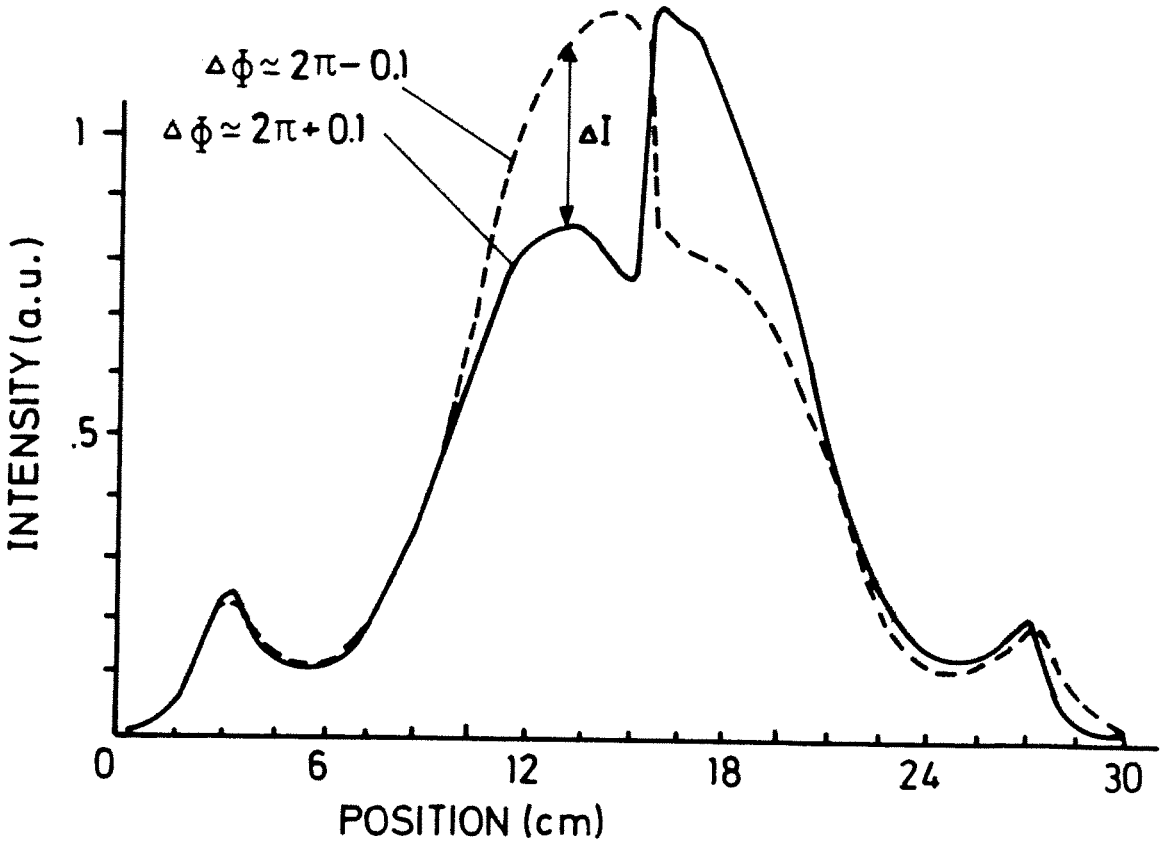
Δφ≃2π−0.1
Δφ≃2π+0.1
ΔI
INTENSITY(a.u.)
1
.5
0
6
12
18
24
30
POSITION (cm)

fig. 3

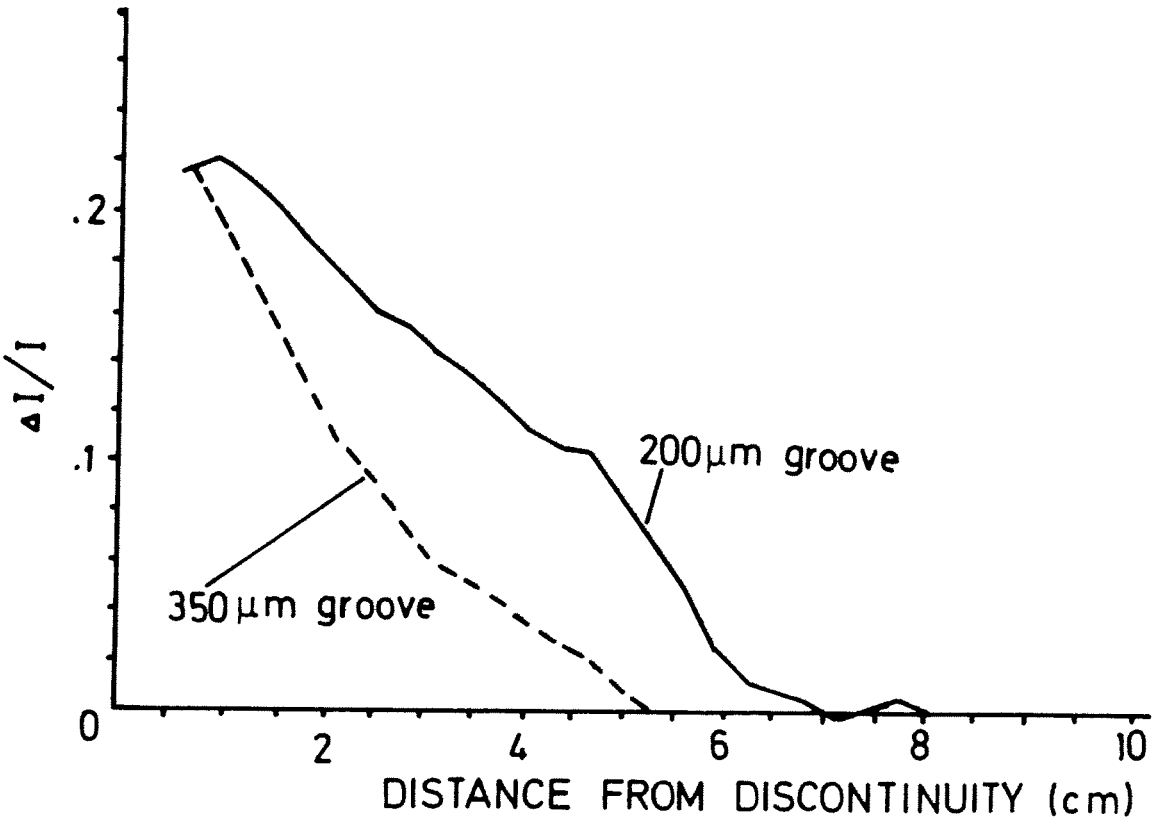
ΔI/I
.2
.1
0
200μm groove
350μm groove
2
4
6
8
10
DISTANCE FROM DISCONTINUITY (cm)

fig. 4

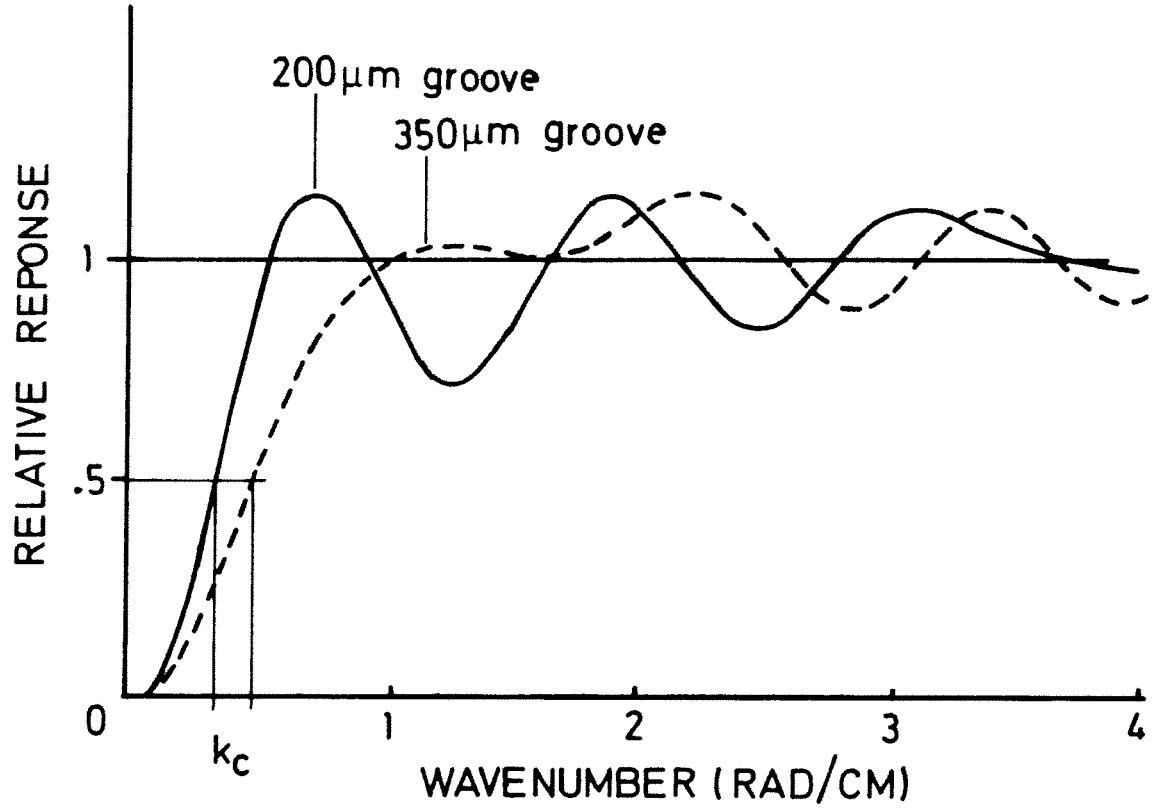
200μm groove
350μm groove
RELATIVE REPONSE
1
.5
0
k_c
1
2
3
4
WAVENUMBER (RAD/CM)

fig. 5

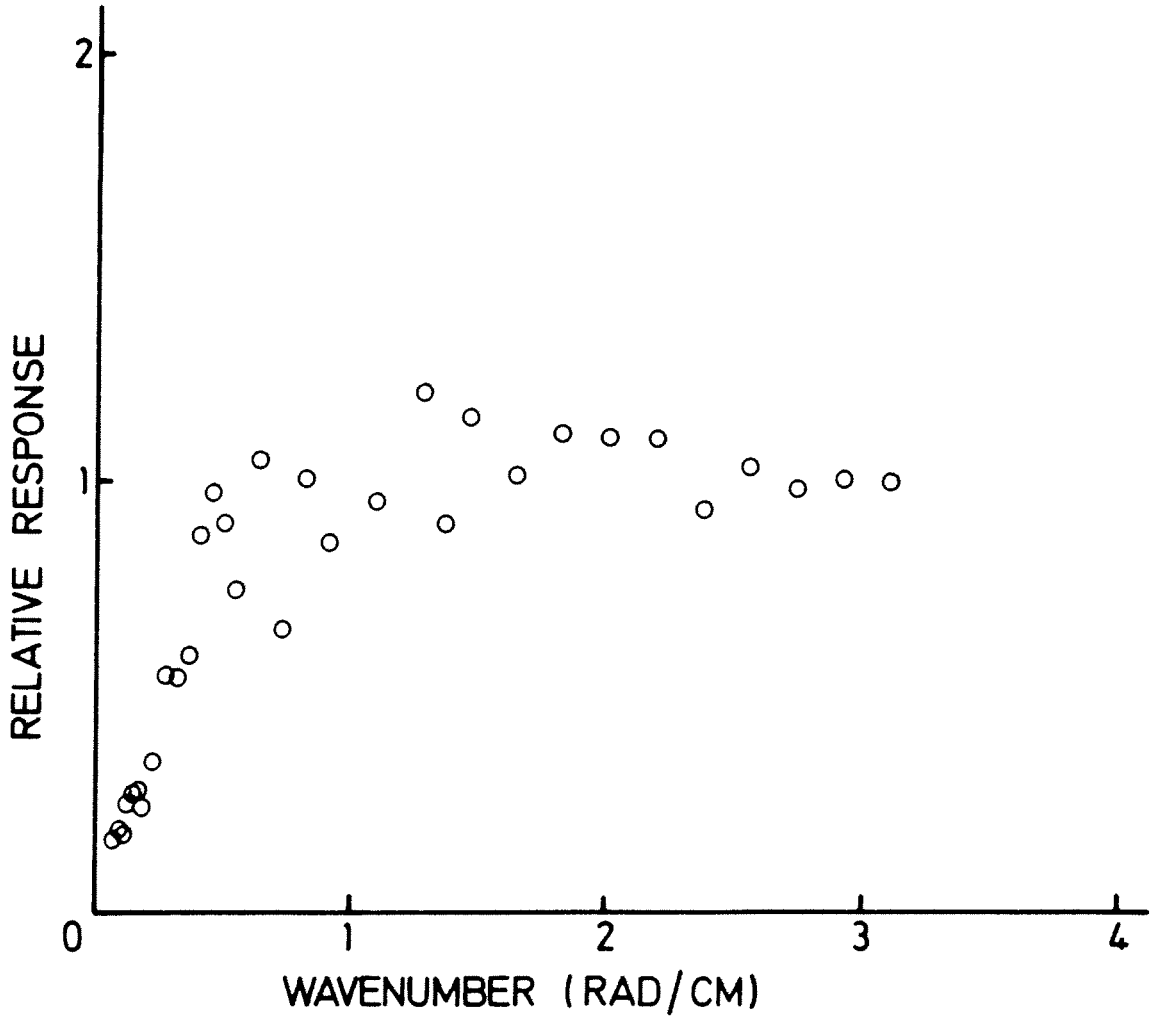
2
1
RELATIVE RESPONSE
0
1
2
3
4
WAVENUMBER (RAD/CM)

fig. 6